Vol. **112** (2007) *ACTA PHYSICA POLONICA A* No. 6

All-Experimental Values of Self-Quenching Cross-Sections for nf States ($n = 5$–8) of Potassium Atoms

M. Głódź[a,*], A. Huzandrov[a], I. Sydoryk[a], J. Szonert[a] and J. Klavins[b]

[a]Institute of Physics, Polish Academy of Sciences
al. Lotników 32/46, 02-668 Warszawa, Poland
[b]Institute of Atomic Physics and Spectroscopy
University of Latvia, Riga, 1586, Latvia

(Received October 17, 2007; in final form November 27, 2007)

All-experimental self-quenching cross-sections σ^q_{nf} are reported for $K(nf)$ states ($n = 5$, 6, 7, 8). The experiment was performed at varied temperatures of K vapour in a spectral cell. Time-resolved fluorescence was observed following pulsed step-wise excitation with dipole and quadrupole transitions $K(4s) \rightarrow K(4p) \rightarrow K(nf)$. The values: $\sigma^q_{5f} = 2.4 \pm 1.7$, $\sigma^q_{6f} = 4.5 \pm 1.4$, $\sigma^q_{7f} = 8.1 \pm 1.8$, and $\sigma^q_{8f} = 18.2 \pm 3.0$ (in units of 10^{-13} cm^{-1}) were obtained from a Stern-Volmer-type plot.

PACS numbers: 32.50.+d, 32.80.Cy

1. Introduction

The first experiment, aimed at determining cross-sections for self-quenching in thermal collisions for nf states of potassium atoms, was reported by our group for $n = 6$, 7, 8 in Ref. [1]. Each cross-section, determined in [1], was based both on a measured value of the effective (increased due to collisional quenching) decay rate of spontaneous fluorescence, corresponding to the temperature of that experiment, and on the theoretical value of natural lifetime adopted from Ref. [2]. In the present paper, we report results of a new experiment, in which cross-sections for $n = 6$, 7, 8 were measured under improved conditions, and the cross-section for $n = 5$ was obtained for the first time. Unlike in [1], in the present experiment we have been able to measure the effective decay rates at various temperatures, and

*corresponding author; e-mail: glodz@ifpan.edu.pl

thus at various number densities of atoms. Therefore, it was possible to obtain all--experimental cross-sections from a Stern–Volmer plot, as described in Sects. 2 and 3. Other essential differences between the two experiments will also be mentioned and discussed below.

In potassium, the $nl \geq 3$ states cluster in a nearly degenerate hydrogen-like n-manifold. Consequently, each $K(nf)$ state is quenched predominantly through the channels of quasi-elastic l-mixing, i.e., of angular momentum-transfer, as described by the following reaction:

$$K(n^2f) + K(4^2s) \rightarrow K(nl > 3) + K(4^2s), \tag{1}$$

since the $nl > 3$ states are the closest neighbours of the $K(nf)$ state, as far as energy is concerned, and they are characterised, among the nl states, by the highest multiplicity. Therefore, in the literature, the total quenching cross-section σ^q_{nf} is identified with the so-called l-mixing cross section being a sum of the contributions characterising particular transfer processes $nf \rightarrow nl > 3$,

$$\sigma^q_{nf} \approx \sigma^{l-\mathrm{mix}}_{nf} = \sum_{l=4}^{n-1} \sigma_{nf\rightarrow nl}. \tag{2}$$

Such quenching/l-mixing cross-sections σ^q_{nf}, thermally averaged, is a subject of interest in the present paper. A comment is due to the fact that, in principle, thermally averaged collisional cross-sections depend on the cell temperature through the temperature dependent (Maxwellian) distribution of the relative atomic velocities, with respect to which the averaging takes place. However, the dependence of σ^q_{nf} on the temperature is expected to be small within the relatively narrow temperature ranges of the experiment centred on *ca.* 410 K, $\pm$30 K for $n = 5$, 6 and $\pm$20 K for $n = 7$, 8 (as listed in Sect. 2). Therefore, we attribute each of the measured cross-sections to the entire respective temperature range. An assumption, that the cross-section can be approximated by a constant, is actually inherent to the data processing method, in which a Stern–Volmer relation is used, see (4) below.

2. Experiment

The experiment was performed in a vapour cell, made of alkali resistant 1720 Corning glass. In the standard preparation procedure, the cell was well outgassed, being backed under vacuum for over one month, 2.5 weeks of which at the highest temperature of 900 K, until the base pressure of less than 1×10^{-8} Torr was reached. Then, the high purity potassium was distilled into it and the cell was sealed off.

The experimental setup is presented in Fig. 1. The cell was heated in a two-chamber oven. Five Ni–NiCr thermocouples, attached to the body of the cell, allowed for the long-term precise stabilisation and control of the temperature. We applied Nesmeyanov formula [3] for the temperature–vapour pressure relation, with respect to the coldest end of the cell containing potassium droplet. The

oven was provided with glass windows to introduce excitation beams to the cell and to allow for the observation of fluorescence. To minimise influence of Earth- and stray-magnetic fields, the cell was surrounded with a double layer of a high permeability foil.

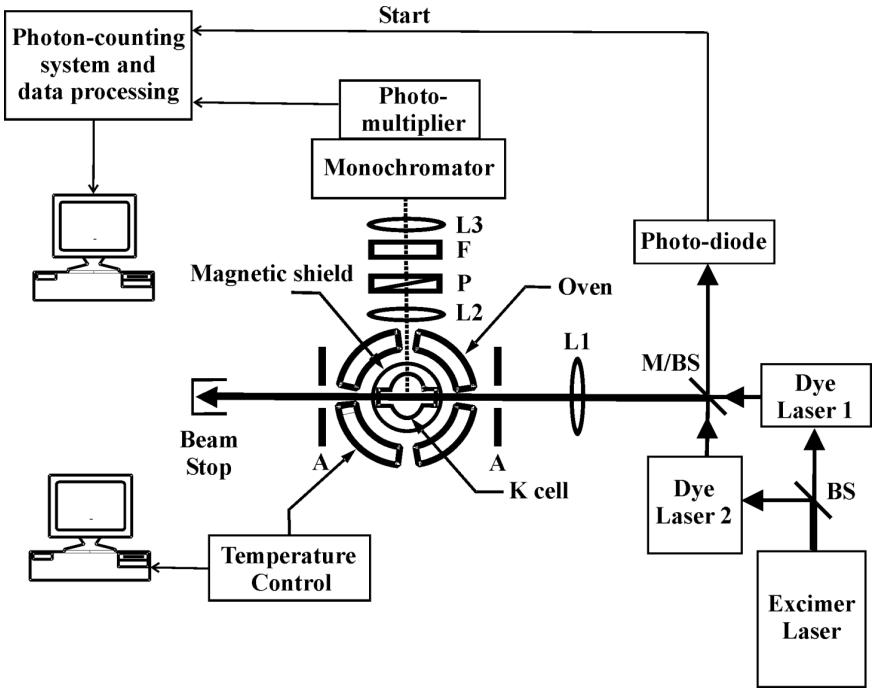

Fig. 1. The scheme of the experimental arrangement. A — apertures, BS — beam-splitter, F — colour glass edge filter, L1-L3 — lenses, M/BS — wavelength selective mirror/beamsplitter, P — linear polarizer.

In order to excite the nf states, a step-wise scheme was applied: the dipole transition $4s_{1/2} \rightarrow 4p_{3/2}$ was followed by the quadrupole transition $4p_{3/2} \rightarrow nf_{5/2,7/2}$ [1, 4, 5]. The cell was irradiated by two vertically polarized, collinear beams of pulsed dye lasers (while in [1] a *cw* external cavity diode laser was applied in the first step). Both dye lasers were pumped by a single excimer laser. The wavelength of one of the lasers was kept at 766.5 nm, for the first-step transition. The another laser was successively tuned to 569.2, 528.7, 506.9, and 493.7 nm, in order to accomplish the quadrupole transitions for $n = 5$, 6, 7, and 8, respectively. The $nf \rightarrow 3d$ fluorescence lines, at 1102.1 nm, 959.7 nm, 890.3 nm, or 850.4 nm, for $n = 5$, 6, 7, 8, respectively, were observed (with the fine structure unresolved) at right angles to the propagation direction of the beams. Fluorescence was collected by the optical system (including polarizer in a "magic angle" configuration to assure that the signal is proportional to the nf state population [6]), and pro-

jected onto the slit of a grating monochromator with spectral slit width of 6 nm. The slits were widely open (to 1.5 mm) to minimise the flight-of-the-view effect [7]. A glass edge filter was inserted across the fluorescence light pathway in front of the monochromator to serve for preliminary spectral filtration. The time-resolved fluorescence signals were registered by means of photon counting technique using a photomultiplier, followed by a fast preamplifier, and a multichannel scaler (MCS) with a 5 ns bin-width. All detected fluorescence lines fall into the infrared region of the spectrum. For the transitions from the $8f$ and $7f$ states, it was still possible to use a photomultiplier with GaAs photocathode (Hamamatsu R 943-02). For transitions from the $6f$ and $5f$ states a photomultiplier with S1 photocathode (FEU 83) was applied. The photomultipliers were cooled down to 200 and 250 K, respectively. The accumulated number of counts per decay curve was of the order of 5×10^4.

The decay curves were measured at various temperatures. The ranges of temperature changes in the excitation region were as following: 378–441 K, 377–440 K, 387–428 K, 387–427 K for $n = 5$, 6, 7, 8, respectively. The temperature of the coldest part of the cell was maintained lower by some degrees, usually by about 5 K, Corresponding ranges of potassium number density N amounted to: $3.7\times10^{11}-2.3\times10^{13}$ cm^{-3}, $2.9\times10^{11}-2.4\times10^{13}$ cm^{-3}, $7.1\times10^{11}-1.1\times10^{13}$ cm^{-3}, $7.1\times10^{11}-1.1\times10^{13}$ cm^{-3}. Our earlier experiment [1] was performed at the temperature of ca. 454 K in the excitation region of the cell, which corresponded to the number density of potassium of *ca.* 3.7×10^{13} cm^{-3}.

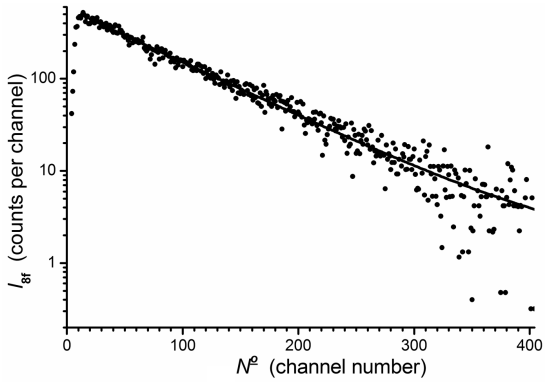

Fig. 2. An example of an experimental decay of fluorescence from $8f$ state with subtracted background (dots). Channel width is 5 ns. The line shows the result of a fit.

Supplementary measurements were also performed in order to enable a careful analysis and minimization of the possible impact of spurious background counts on the results. Background signals with the second-step laser detuned from the $4p_{3/2}-nf_{5/2,7/2}$ line were registered with resolution in time. An example of a fluorescence decay signal, from which the background of this kind was subtracted,

is given in Fig. 2 (dots). Emission spectra were measured in the near infrared, comprising the $8f-3d$ line and its neighbourhood.

3. Data processing

In a data processing procedure of numerical fitting, a single-exponential character of the fluorescence decay was assumed. This has been justified by an analysis based on rate equations. In the estimates, the conditions of the present experiment as well as the results of the supplementary spectral measurements were taken into account. The residual background in the signal was approximated by introducing modifications to the single exponential function. Usually a constant background was assumed. For $n = 7$, 8 we also attempted to add another single exponential function to the fitted one. This resulted in either no effect, or a little effect, on the obtained lifetimes. The line in Fig. 2 is an example of a fitted decay.

Finally, the decay parameter Γ_{nf}, corresponding to a given temperature of the experiment, was obtained by using the procedure of a two-step averaging. The average of decay parameters fitted to an experimental decay, whose initial channels were successively truncated, was taken for the result of each approach. The average of such results was considered to be the final Γ_{nf} value at this temperature.

At any temperature above 0 K the effective decay rate Γ_{nf} exceeds the natural decay rate $1/\tau_{nf}$ of the nf state population (τ_{nf} is the natural lifetime of the state), by the sum of the temperature dependent contributions: the rate $\sigma^q_{nf}Nv$ of collisional quenching, and the rate Γ_n^{BBR} of all processes of absorption and stimulated emission from the nf state induced by thermal radiation (index BBR means "blackbody radiation")

$$\Gamma_{nf} = 1/\tau_{nf} + \sigma^q_{nf}Nv + \Gamma_n^{\mathrm{BBR}}, \tag{3}$$

symbol N denotes the number density of the ground state atoms (which is practically equal to the number density of all atoms), and $v = (8kT/\pi\mu)^{1/2}$ is the mean relative velocity of the colliding pair, namely of the potassium atoms in the excited state and in the ground state; μ is their effective mass.

Each of the measured Γ_{nf} values was first corrected for the thermal radiation effect, $\Gamma_n^{\mathrm{corr}} = \Gamma_n - \Gamma_n^{\mathrm{BBR}}$, by adopting for Γ_n^{BBR} values available from Ref. [2] interpolated to the temperature at which the particular decay was registered. For the states of interest, within the temperature ranges of the experiment, the corrections are small, and in the percentage of the Γ_{nf} values they amount to 0.3–0.5, 1.0–1.3, 2.1–2.4, 2.4–3.3, for $n = 5$, 6, 7, 8, respectively.

According to Eq. (3), Γ_n^{corr} rates are expected to be linearly dependent on Nv

$$\Gamma_{nf}^{\mathrm{corr}} = 1/\tau_{nf} + \sigma^q_{nf}Nv. \tag{4}$$

By fitting the Stern–Volmer relation (4) to the experimental dependence of Γ_n^{corr} upon Nv, the collisional quenching cross-sections σ^q_{nf}, as well as the natural lifetimes τ_{nf} were obtained. The Stern–Volmer plots for all investigated $K(nf)$ states are presented in Fig. 3. The points represent the experimental Γ_n^{corr} values, and

lines are the results of the fits. Errors in $\Gamma_n^{\rm corr}$, marked in Fig. 3, correspond to the uncertainties coming from the fitting procedure of obtaining Γ_{nf}. The contribution of each experimental point to the minimized χ^2 function was weighted by the inverse of the square of such an uncertainty in Γ_{nf}.

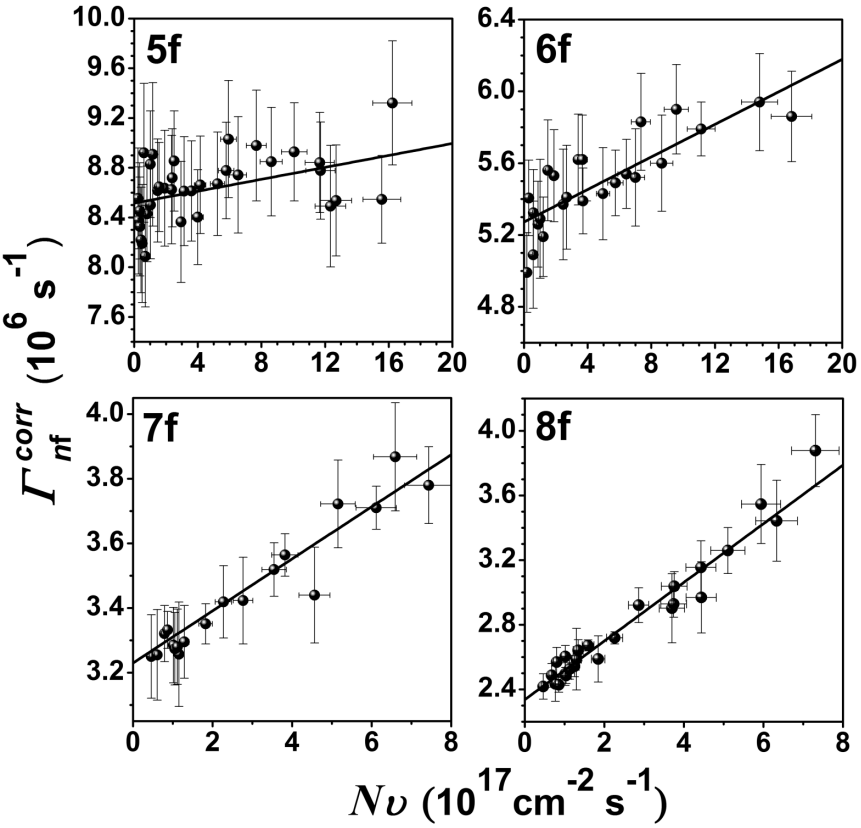

Fig. 3. Stern–Volmer plots for $K(nf)$ states with $n = 5$–8. Points are the experimentally determined fluorescence rates corrected for the effect of thermal radiation present in the cell. Lines are the results of the fits of the Stern–Volmer relation.

In estimating errors in $N\upsilon$, marked in Fig. 3, we took into account a 0.5 K uncertainty, with which the cell temperature was known.

The lifetime values determined together with the quenching cross-sections and corresponding theoretical lifetimes, calculated by using the relativistic all--order method, are reported in [8].

4. Results and discussion

The obtained σ_{nf}^q results are collected in Table. The values from Ref. [1] are also displayed. To our knowledge, no relevant theoretical values have been

reported in the literature. However, the theoretical treatments (e.g., the ones reviewed in [9], section 5.2.5) predict that cross-sections for l-mixing in collisions of Rydberg atoms with neutral particles are of the order of geometrical cross--sections, providing the Rydberg atoms are in states with n values low enough, and such are the potassium Rydberg atoms in our experiment. As stated in Sect. 1, the measured quenching cross-sections σ^q_{nf} are practically the l-mixing cross-sections, $\sigma^q_{nf} \approx \sigma^{l-\mathrm{mix}}_{nf}$, therefore we have included, for comparison, the geometrical cross--sections in the last column of Table. The geometrical cross-sections are defined as in [1]. As expected, the values measured in both experiments roughly correlate with the geometrical cross-sections.

TABLE

Quenching (l-mixing) cross-sections for $K(nf)$ states ($n = 5$–8) measured in this experiment and the ones obtained in the earlier experiment [1], and the geometrical cross-sections for $K(nf)$ atoms. All values are in units of 10^{-13} cm^2.

Potassium	Quenching cross-section		Geometrical
nf state	This experimental	Ref. [1]	cross-section
$5f$	2.4±1.7	–	1.3
$6f$	4.5±1.4	3.6±2.2	2.7
$7f$	8.1±1.8	4.2±2.6	5.1
$8f$	18.2±3.0	8.0±4.6	8.8

The uncertainty in each result σ^q_{nf} of the present experiment is a sum of two components: the one is the statistical error of the fit of the Stern–Volmer relation $\delta^{\mathrm{fit}}_{nf}$ and the other is an estimated error due to uncertainties in Nv values $\delta^{\mathrm{fit}}_{nf}$. Their contributions in the percentage of σ^q_{nf} amount to: $\delta^{\mathrm{fit}}_{5f} = 63$, $\delta^{\mathrm{fit}}_{6f} = 24$ $\delta^{\mathrm{fit}}_{7f} = 13$, $\delta^{\mathrm{fit}}_{8f} = 8$ and $\delta^{Nv}_{5f} = 8$, $\delta^{Nv}_{6f} = 8$, $\delta^{Nv}_{7f} = 9$, $\delta^{Nv}_{8f} = 9$. Other sources of uncertainty, such as: the inaccuracy in MCS calibration, a possible error in calculation of the BBR corrections from [2] (these corrections themselves, as listed in Sect. 3, are rather small), as well as an error introduced to these corrections by our interpolation procedure, give much smaller contributions and we have neglected them.

The cross-sections from Table are plotted in Fig. 4 as a function of n. The values of the present experiment are marked by full squares, while the ones from [1] are marked by open squares. The circles symbolise the respective geometrical cross-sections. The line is drawn only to guide the eye.

All values for from [1] are smaller than the respective values measured in the present experiment, and the relative deviation tends to increase with increasing quantum number n. Only σ^q_{6f} of [1] approaches the value of the present experiment

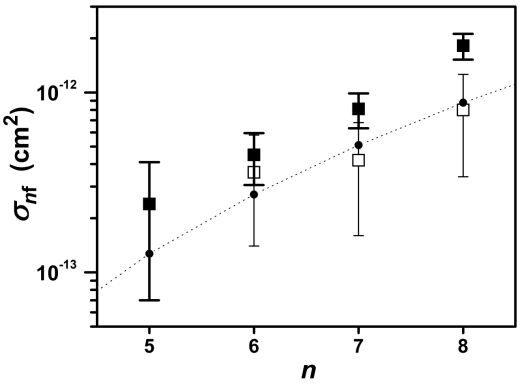

Fig. 4. The quenching cross-sections of the $K(nf)$ states from Table plotted with their uncertainties as a function of principal quantum number n. Full squares are for the results measured in this experiment, the open squares for the results of [1]. The geometrical cross-sections, marked by circles, are added for comparison.

well within the overlap of both results uncertainties. Results for comparison are available in three pairs only; also uncertainties, especially those given with the values of experiment [1], are quite big. Yet, the character of divergence (observed in Fig. 4 and in Table) between the results in pairs seems to be not merely of statistical origin, and is therefore worth being analysed.

Theoretical lifetimes of Theodosiou [2], used in [1] to derive the cross-sections from the decay rates, are bigger than the respective experimental lifetimes of [8] determined together with the cross-sections of this paper. According to Stern–Volmer relation (4), this should produce σ^q_{nf} obtained in [1], which are slightly bigger than the σ^q_{nf} values of the present experiment. Therefore, the differences cannot be explained in this way.

By reviewing experimental conditions, we have decided that the main factor, which should be blamed for the differences in the results, is the temperature of the experiment [1] (for the temperature values see Sect. 2), which was probably too high. In the present experiment we have undertaken various measures, like estimates based on rate equations, analysis of the background in the signal, and analysis of some emission spectra (Sects. 2 and 3, and Ref. [8]). The goal was to verify that up to the highest Nv values in the experiment, the single-exponential character of the decay was not distorted in a significant way due to some spurious effects. Indications were found that, at least for $n = 8$, the acceptable limit of Nv was being approached in the experiment.

One of such spurious effects could be a backstream of collisional repopulation from other states of the same hydrogen-like manifold. The states $nl > 3$ are characterised by longer lifetimes than the nf state lifetime. Therefore, the repopulation would result in an admixture to the nf state fluorescence of components with decay rates smaller than Γ_{nf}. Then, if a single exponential function is erro-

neously assumed in fitting, the decay parameter thus obtained, would appear to be smaller than the actual Γ_{nf} rate. (In the limit of high enough Nv values, total l-mixing takes place and indeed fluorescence from an nf state decays according to a single exponential function, but with the decay rate being the statistical average of all decay rates of $l \geq 3$ states.) We suspect that this could have been the case with experiment [1]. Not only the direction of change between the values of the two experiments, but also the increase with n in the relative difference agree with such a conclusion. At a given temperature of the experiment this effect should become more significant with increasing n, as the number of the states $l > 3$ of the manifold and their multiplicity increase with rising n.

Another effect, which, in a similar way, could manifest itself in too small fitted Γ_{nf} values, would be delayed cascading populating the nf state from some higher states. These higher states could have been populated, e.g., via pulsed two--photon ionisation followed by recombination. Owing to our careful control over the experimental conditions and over data processing in the present experiment, we believe that no such processes have spoiled the results. As far as the experiment [1] is concerned, it is quite difficult to speculate about the presence or absence of the processes of such kind, because what counts in this case, is not only a different temperature, but also a different kind of the first-step laser used.

5. Conclusions

In conclusion, we report the first obtained all-experimental values for thermally averaged quenching cross-sections σ^q_{nf} for nf states of potassium (with $n = 5$–8) in collisions with ground state potassium atoms. To our best knowledge, no corresponding theoretical values are available in the literature. It is expected that for these hydrogen-like states, quenching proceeds almost entirely via channels $K(nf) \rightarrow K(nl > 3)$, i.e., through l-mixing channels. Unlike the l-mixing collisions of alkali atom with inert gas atoms, such alkali–alkali collisions are rarely interpreted by theorists. The measured σ^q_{nf} values are close to geometrical cross-sections (on average, σ^q_{nf} are bigger by 80%), which are defined mainly by the size of the cloud of the nf state electron. This may indicate that the interaction of the ground state potassium atom with the excited electron of the perturbed nf state atom plays the main role in the collisional process. Such e^--perturber interaction was assumed in an early model developed by Prunelé and Pascale [10] and applied for l-mixing of rubidium nf states, as mentioned in [11]. However, the possibility of interaction with the core should not be excluded, as can be inferred from more recent calculations on l-mixing [12].

Acknowledgments

The authors acknowledge a partial support by the EU-FP6-TOK project LAMOL (contract MTKD-CT-2004-014228).

References

[1] M. Głódź, A. Huzandrov, J. Klavins, I. Sydoryk, J. Szonert, S. Gateva-Kostova, K. Kowalski,*Acta Phys. Pol. A* **98**, 353 (2000).

[2] C.E. Theodosiou,*Phys. Rev. A* **30**, 2881 (1984).

[3] A.N. Nesmeyanov, *Vapor Pressure of the Chemical Elements*, Elsevier, Amsterdam 1963.

[4] J. Szonert, B. Bieniak, M. Głódź, M. Piechota,*Z. Phys. D* **33**, 177 (1995).

[5] P.F. Liao, J.E. Bjorkholm,*Phys. Rev. Lett.* **36**, 1543 (1976).

[6] P. Hannaford, R.M. Lowe,*Opt. Eng.* **22**, 532 (1983).

[7] L.J. Curtis, P. Erman,*J. Opt. Soc. Am.* **67**, 1218 (1977).

[8] M. Głódź, A. Huzandrov, M.S. Safronova, I. Sydoryk, J. Szonert, J. Klavins, submitted to *Phys. Rev. A* (2007).

[9] I.L. Beigman, V.S. Lebedev,*Phys. Rep.* **250**, 95 (1995).

[10] E. de Prunelé, J. Pascale,*J. Phys. B* **12**, 2511 (1979).

[11] M. Hugon, F. Gounand, P.R. Fournier, J. Berlande,*J. Phys. B* **12**, 2707 (1979).

[12] H. Liu, B. Li,*J. Phys. B* **27**, 497 (1994).